Immune Landscape and Prognostic Significance of Gene Expression Profiles in Bladder Cancer: Insights from Immune Cell Infiltration and Risk Modeling

Ye Zhou[1], Hengyan Zhang[2], Heguo Yan[1,3], Pingxing Han[4], and Yangwen Liu[4]

[1] Department of Endocrinology, Zhaotong Hospital of Traditional Chinese Medicine, Zhaotong, China
[2] Department of Dermatology, Zhaotong Hospital of Traditional Chinese Medicine, Zhaotong, China
[3] Clinical Medical College, Yunnan University of Chinese Medicine, Kunming, China
[4] Department of General Surgery, Zhaotong Hospital of Traditional Chinese Medicine, Zhaotong, China

ABSTRACT

To explore the immunological underpinnings and prognostic potential of gene expression profiles in bladder cancer through comprehensive analyses of The Cancer Genome Atlas (TCGA) data.

We used the TCGA data to identify differentially expressed genes (DEGs) and performed enrichment analysis to reveal the related biological pathways. Meanwhile, the least absolute shrinkage and selection operator (LASSO) algorithm was adopted to develop a prognostic model. Then we evaluated the performance of the model in both TCGA and GSE13507 datasets. Furthermore, we conducted a comprehensive investigation on the feature genes utilized in model construction, encompassing both gene expression profiling and survival analysis. Finally, immune infiltration analysis and drug sensitivity analysis were applied to elucidate the immunological basis of the disease and provide potential therapeutic strategies.

We identified a total of 837 DEGs, with a focus on immune-related genes. Using the LASSO algorithm, we developed a prognostic model incorporating seven key genes—*NXPH4*, *FAM110B*, *GPC2*, *STXBP6*, *CYP27B1*, *GARNL3*, and *PTGER3*—which demonstrated strong predictive accuracy in both TCGA and GSE13507 datasets. Moreover, immune infiltration analysis revealed a higher abundance of M0 and M2 macrophages in high-risk patients, suggesting that macrophage polarization could be a potential therapeutic target to modulate the immune microenvironment. Drug sensitivity analysis further suggested that high-risk patients exhibit differential responses to several chemotherapy agents, with potential therapeutic implications.

This study constructed an effective prognostic model, providing new insights and potential therapeutic targets for the personalized treatment of bladder cancer, which needs further validation.

Keywords: Bladder cancer; Immune cell infiltration; LASSO; Macrophage polarization; Prognostic risk model

Corresponding Author Yangwen Liu, MD;
Department of General Surgery, Zhaotong Hospital of Traditional Chinese Medicine, Zhaotong, Yunnan 657000, China. Tel: (+86 1577) 02577 59, Fax: (+86 0870) 2233 331, Email: liuywpwk@163.com

*The first and second authors contributed equally to this study

INTRODUCTION

Bladder cancer is a common malignancy of the urinary system worldwide.[1] It primarily affects older adults, with men diagnosed more frequently than

women. The incidence of bladder cancer varies by region, with higher rates in developed countries, possibly due to longer life expectancy and a higher prevalence of risk factors such as smoking and occupational exposure.[2] Clinically, bladder cancer has a high recurrence rate, and treatment strategies vary depending on the disease stage, with immunotherapy playing a crucial role in advanced cases.[3] Early-stage patients typically have a better quality of life than those with advanced disease, making early detection critical for achieving favorable outcomes.

Biomarkers play an increasingly important role in the diagnosis, prognosis, and treatment of bladder cancer. Biomarkers not only improve early detection rates but also provide crucial information for developing personalized treatment plans. For instance, urinary biomarkers such as nuclear matrix protein 22 (NMP22) and fibroblast growth factor receptor 3 (FGFR3) mutation testing can aid in early diagnosis.[4] Prognostic markers, such as p53 protein and Ki-67, can predict disease progression and recurrence risk, whereas programmed death-ligand 1 (PD-L1) expression levels are key in selecting and evaluating the effectiveness of immunotherapy.[5] The application of these biomarkers not only helps improve patient prognosis but also enhances treatment effectiveness, thereby improving the overall quality of life.

Prognosis is a core aspect of disease diagnosis and patient management.[6] Clinicians predict patient outcomes based on disease characteristics.[7] With advancements in Next-generation sequencing (NGS) technology, the accuracy and personalization of prognostic models have significantly improved. NGS enables a comprehensive understanding of tumor genomic features, including gene mutations, copy number variations, and gene expression profiles, which are crucial for assessing disease prognosis.[8] These findings not only enhance our understanding of tumor biology but also identify potential prognostic biomarkers that can improve predictive accuracy and guide personalized treatment.[9]

The tumor microenvironment (TME) of bladder cancer significantly influences its growth, invasion, and metastasis. Immune checkpoint inhibitors (ICIs), including Bacillus Calmette-Guérin (BCG), are effective treatments for bladder cancer through modulation of the tumor immune microenvironment. Macrophages, as the most prevalent infiltrative inflammatory cells within the bladder cancer TME, play

a crucial role in the disease's initiation and progression. Once released from the bone marrow, monocytes enter the bloodstream and are attracted to the TME by various chemokines secreted by tumor cells, such as macrophage colony-stimulating factor (M-CSF), C-C motif chemokine ligand 2 (CCL2), CCL5, CXCL12, and vascular endothelial growth factor (VEGF), where they differentiate into tumor-associated macrophages (TAMs).[10] TAMs exhibit significant plasticity and become activated in response to microenvironmental signals, differentiating primarily into two distinct phenotypes: classically activated macrophages (M1 phenotype) and alternatively activated macrophages (M2 phenotype). M1 macrophages are mainly involved in the immune response of type I helper T cells (Th1), which are responsible for inducing inflammation and eliminating bacteria and tumor cells. In contrast, M2 macrophages primarily participate in the Th2 type immune response, which can suppress inflammation, promote wound healing, and support tumor progression. This contributes to the formation of various tumors and is associated with poor prognosis, thus, M2 macrophages are considered protumor macrophages.[11]

This study was based on The Cancer Genome Atlas (TCGA) bladder cancer data and began by identifying differentially expressed genes related to bladder cancer, followed by functional enrichment and survival analysis to select prognostic genes. Subsequently, a risk assessment model was constructed using the least absolute shrinkage and selection operator (LASSO) algorithm based on these differentially expressed genes, dividing patients into high and low-risk groups. Finally, comprehensive analyses of immune cell infiltration and small-molecule drug sensitivity were conducted for both groups. Through these analyses, this study aimed to explore in depth the prognostic mechanisms of bladder cancer and provide robust support for personalized treatment and prognostic management of bladder cancer patients. Ultimately, by constructing and validating effective risk assessment models, this study seeks to provide scientific evidence for clinical decision-making and to improve treatment outcomes and quality of life for patients.

MATERIALS AND METHODS

Data Acquisition
Gene expression and clinical data for patients with bladder cancer were downloaded from the TCGA

website (https://portal.gdc.cancer.gov/). This dataset included gene expression data from 414 bladder cancer patients and 19 corresponding normal tissue samples. Duplicate samples and those with a total survival time of less than 10 days were excluded. mRNA expression and clinical data from GSE13507 were obtained from the Gene Expression Omnibus (GEO) database (https://www.ncbi.nlm.nih.gov/geo/), which included 165 primary bladder cancer samples and 58 adjacent normal bladder mucosa samples, serving as the validation set. Prior to further analysis, RNA sequencing data underwent preprocessing to guarantee data quality and conformity. Samples were selected based on having complete clinical and genomic data, along with a sequencing depth of at least 30x. Those with low quality or a missing data rate exceeding 10% were excluded. Before further analysis, the data were standardized and normalized to ensure comparability between different samples. This normalization process takes sequencing depth and gene length into account, thereby reducing batch effects and variability.

Differential Expression Analysis

We first extracted mRNA data from TCGA expression data and performed gene ID conversion using the `trans_exp` function from the `Tinyarray` package, specifying parameters `mrna_only=True`, `lncrna_only=False`, resulting in the final mRNA expression matrix. The mRNA expression matrix was then converted into a `DESeqDataSet` object using the `DESeqDataSetFromMatrix` function in the DESeq2 package, which integrates expression data with sample information.[12] Before performing differential expression analysis, the expression matrix was normalized using the `estimateSizeFactors` and `count` functions. Differential expression analysis was conducted using the `DESeq` function, applying thresholds of |log2FC|>1 and false discovery rate (FDR)<0.05 to identify biologically significant differentially expressed genes. Finally, volcano plots were created using the `ggplot2` function, and heatmaps of the top 20 significantly upregulated and downregulated genes were plotted using the `pheatmap` function.

Functional Enrichment Analysis

Functional enrichment analysis of the differentially expressed genes was performed using the `ClusterProfiler` package.[13] First, the gene IDs were converted from Gene Symbol to Entrez ID using the

`bitr` function. Gene ontology (GO) enrichment analysis was conducted by mapping differentially expressed genes to the Gene Ontology database to determine their enrichment in Molecular Function (MF), Cellular Component (CC), and Biological Process (BP). The `enrichGO` function was used with the species set to "org.Hs.eg.db" to obtain the GO enrichment results. Kyoto Encyclopedia of Genes and Genomes (KEGG) enrichment analysis was performed using the `enrichKEGG` functions. The Enrichment results were visualized using a `barplot` function.

Construction of Prognostic Model

The LASSO Cox regression model combines L1 regularization with the Cox proportional hazards model for survival analysis. First, the relationship between differentially expressed genes and bladder cancer prognosis was analyzed using the Kaplan-Meier method (KM) and Cox survival analysis for each gene, with a threshold set at $p<0.05$. The intersection of the KM and Cox results identified the final prognostic-related differentially expressed genes. The selected genes were then used to build a model using the `glmnet` package. A key step in LASSO Cox regression is selecting an appropriate regularization parameter λ, which controls the strength of L1 regularization and directly affects the model complexity and variable selection stringency. The optimal λ value was chosen using cross-validation, resulting in the final model, which was then evaluated using the validation set GSE13507. The `timeROC` package was used to assess the model's 1-, 3-, and 5-year predictive performance.

Immune Infiltration Analysis

Immune infiltration analysis is a crucial method for studying the composition and function of immune cells in the tumor microenvironment. We used the Cell-type Identification by Estimating Relative Subsets of RNA Transcripts (CIBERSORT) algorithm to assess the relative abundance of different immune cell subtypes in bladder cancer patient samples.[14] The expression matrix was first standardized using transcripts per million (TPM) conversion. Immune infiltration analysis was performed based on the leukocyte signature matrix 22 (LM22) gene expression signature of the known immune cell subtypes. The abundance of immune cell subtypes was compared based on the constructed prognostic model to evaluate their correlation with the prognostic model.

Small Molecule Drug Sensitivity Analysis

Small-molecule drug sensitivity analysis is a key step in drug development and in personalized medicine. The Genomics of Drug Sensitivity in Cancer (GDSC) database provides valuable data resources for this analysis, including sensitivity and response data of tumor cell lines to small molecules, which supports the prediction of patient responses to drugs. We used the `oncoPredict` package to predict the sensitivity of patients to small molecules based on the GDSC database. The `oncoPredict` package includes pretrained models for the GDSC database, which combines gene expression features of cancer cell lines with drug sensitivity data to predict drug responses in bladder cancer patients. The model calculated the sensitivity scores for various small molecules for each patient. Finally, the predicted sensitivity scores were combined with the prognostic model to identify potential therapeutic options and to explore the association between drug sensitivity and the prognostic model.

RESULTS

Identification of Differentially Expressed Genes in Bladder Cancer

First, we filtered out mRNA from the TCGA bladder cancer sample expression data, resulting in 19,474 mRNAs. Principal Component Analysis (PCA) was performed on the filtered expression matrix, revealing distinct differences in gene expression features between tumor and normal samples. PC1 captured the most significant source of variance between the two groups, while PC2 represented the secondary source of variation. Then we visualized the distribution of samples using PC1 and PC2 as the coordinate axes. Together, PC1 and PC2 explained 16.8% of the variance between the two groups (Figure 1A). The scatter plot of the sample distribution showed distinct patterns between bladder cancer and adjacent normal samples (Figure 1B). Next, differential expression analysis between bladder cancer and adjacent normal samples identified 837 differentially expressed genes, with 599 genes downregulated and 238 genes upregulated. A volcano plot was generated based on Log2FC and the *p* value of each gene (Figure 1C). Finally, to visually assess the expression patterns of the differentially expressed genes in the samples, a heatmap was created, which confirmed that the expression patterns of these differentially

expressed genes were consistent with the results of the differential analysis (Figure 1D).

Functional Enrichment Analysis of Differentially Expressed Genes

To explore the functions of differentially expressed genes associated with bladder cancer, we performed Gene Ontology (GO) enrichment analysis and visualized the results using a bubble plot. The analysis revealed that the primary molecular functions of these differentially expressed genes included tubulin, microtubule, glycosaminoglycan, sulfur compound, and heparin binding (Figure 2A). The genes were mainly localized to the collagen-containing extracellular matrix, contractile fibers, myofibrils, sarcomeres, and centromeric regions of chromosomes (Figure 2B). The biological processes involving these genes included muscle system processes, organelle fission, muscle contraction, nuclear division, and chromosome segregation (Figure 2C). KEGG pathway enrichment analysis was conducted to study the association between differentially expressed genes and pathways. The results indicated that the enriched pathways included hypertrophic cardiomyopathy, dilated cardiomyopathy, arrhythmogenic right ventricular cardiomyopathy, the cell cycle, cyclic guanosine monophosphate-cGMP-dependent protein kinase (cGMP-PKG) signaling pathway, and vascular smooth muscle contraction (Figure 2D).

Construction of the Bladder Cancer Prognostic Model

First, we assessed the relationship between the differentially expressed genes and the prognosis of patients with bladder cancer. Using KM and Cox regression analyses, we identified 231 genes associated with prognosis from KM analysis and 215 genes from Cox regression analysis. The intersection of these results yielded 137 genes (Figure 3A). Next, we used the LASSO algorithm on the TCGA dataset to select important genes. The results showed that as the λ increased, some less important genes were removed from the model. Ultimately, seven genes were selected for inclusion in the model: NXPH4 (log2FC=2.81, FDR<0.001), FAM110B (log2FC=−1.65, FDR<0.001), GPC2 (log2FC=2.27, FDR<0.001), STXBP6 (log2FC=−1.97, FDR<0.001), CYP27B1 (log2FC=1.99, FDR<0.001), GARNL3 (log2FC=−1.35, FDR=0.001), and PTGER3 (log2FC=−1.83, FDR=0.002), as shown in Figure 3B–C. Then we performed Multivariate Cox regression analysis to determine the correlation between the seven genes in

the model and prognosis, and plotted a forest plot. Among these, NXPH4, STXBP6, and PTGER3 had hazard ratios (HR1, indicating that they are risk factors. Conversely, GPC2, CYP27B1, and GARNL3 had HRs less than 1, indicating that they were protective factors. FAM110B gene was not significantly correlated with prognosis (Figure 3D). Using the constructed prognostic model, we calculated the risk score for each patient with bladder cancer. Based on the median risk score of all patients, we divided them into high-risk and low-risk groups. Next, we created a heatmap of the expression of these seven genes in the TCGA samples. The results showed that NXPH4, STXBP6, FAM110B, and PTGER3 were upregulated in high-risk groups, whereas CYP27B1, GPC2, and GARNL3 were downregulated (Figure 3E).
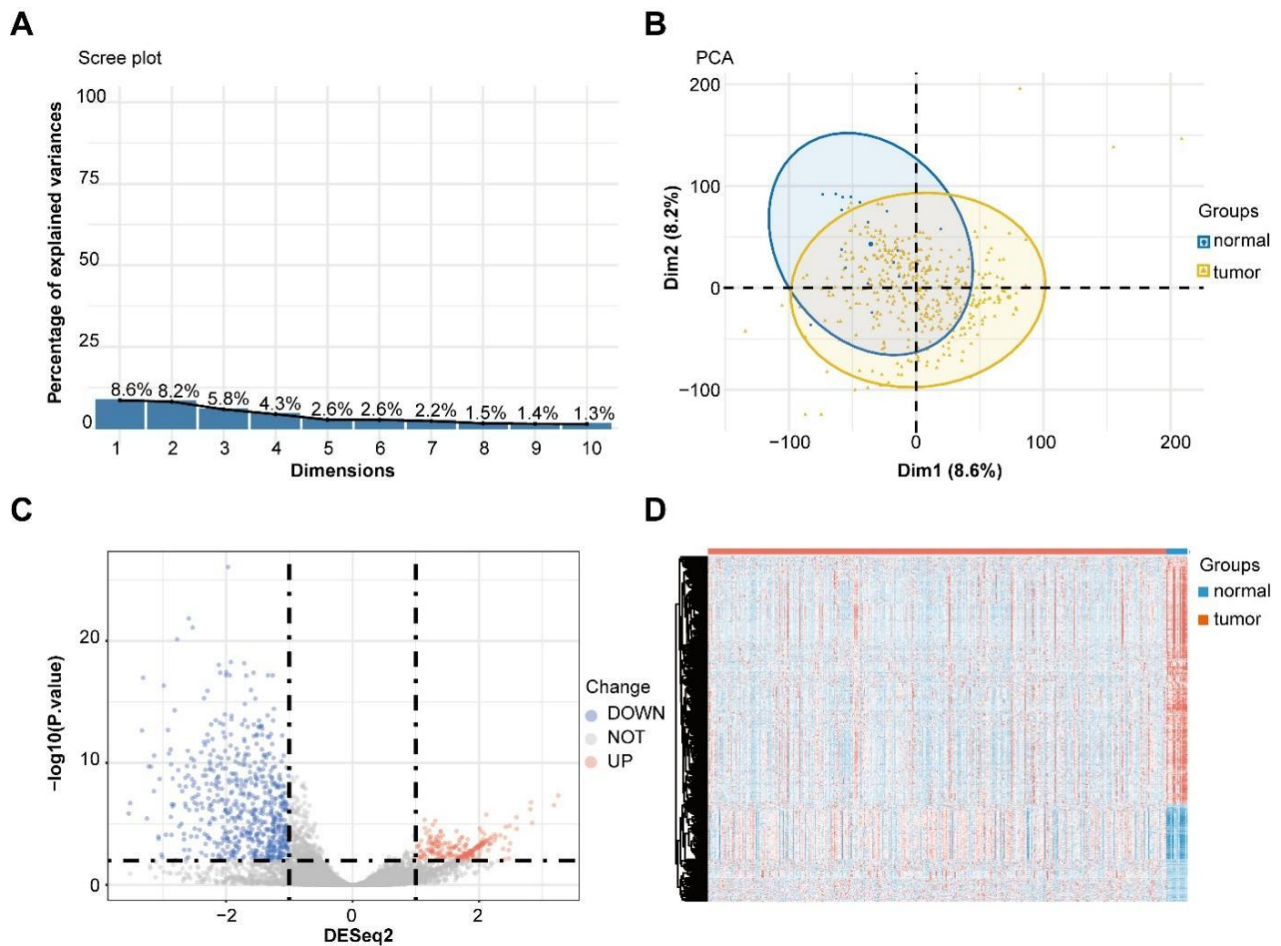

Figure 1. Identification of Differentially Expressed Genes in Bladder Cancer. A. Principal component analysis (PCA) analysis of mRNA expression data from The Cancer Genome Atlas (TCGA) bladder cancer samples. Principal components 1 and 2 (PC1 and PC2) account for 16.8% of the variance in the samples. B. Scatter plot showing the distinct distribution patterns of bladder cancer and adjacent normal samples. C. Volcano plot of differentially expressed genes, highlighting 238 upregulated and 599 downregulated genes based on log2 fold change (Log2FC) and *p* value. D. Heatmap displaying expression patterns of differentially expressed genes in bladder cancer versus adjacent normal samples, consistent with the differential expression results.
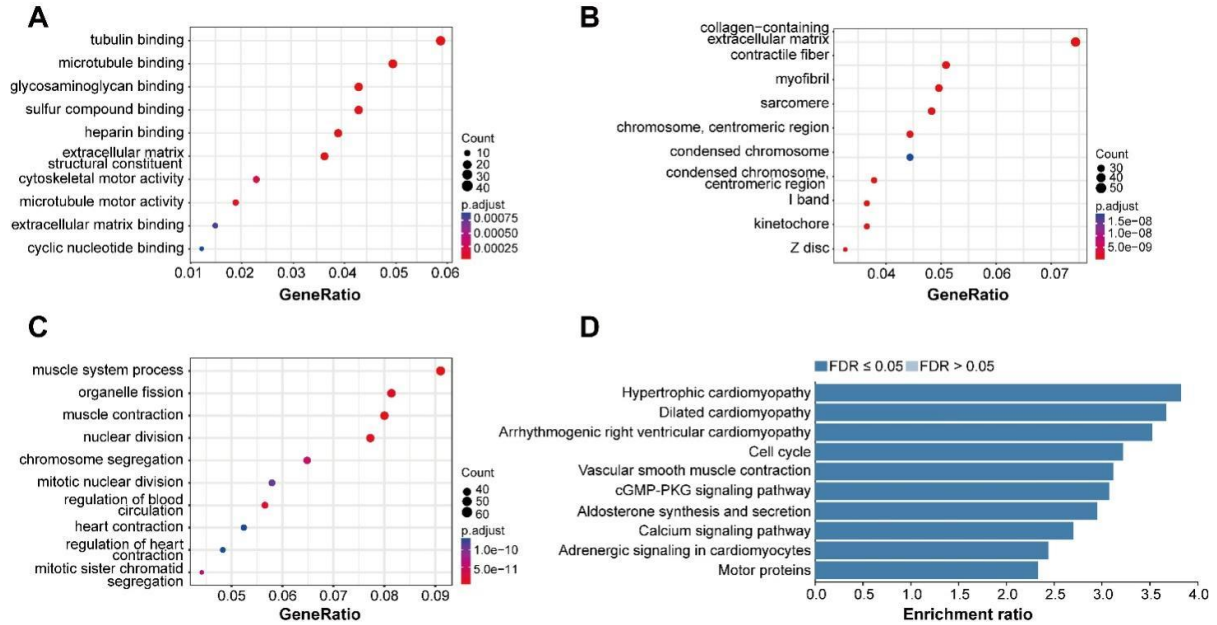
Figure 2. Functional Enrichment Analysis of Differentially Expressed Genes. A. Gene Ontology (GO) enrichment bubble plot showing the primary molecular functions of differentially expressed genes. B. GO enrichment bubble plot of cellular localization. (C) GO enrichment bubble plot of biological processes. D. Kyoto Encyclopedia of Genes and Genomes (KEGG) pathway enrichment analysis reveals significant pathways.
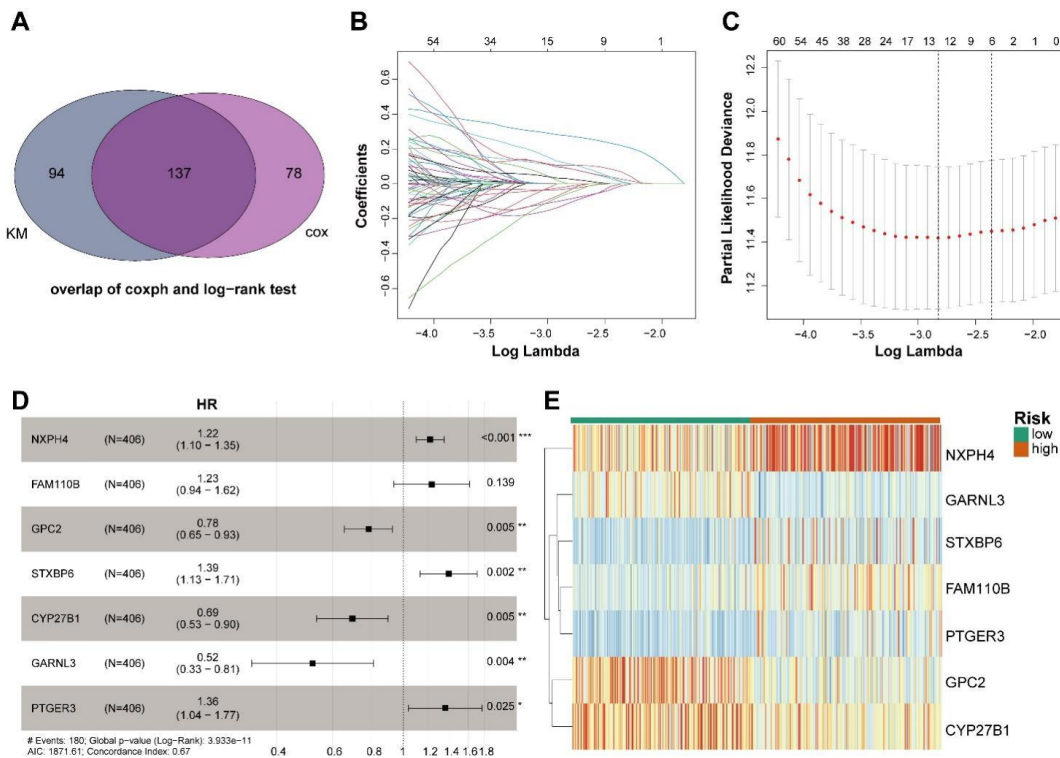

Figure 3. Construction of a prognostic model for bladder cancer. A. Venn diagram showing 137 genes common to Kaplan-Meier and Cox regression analyses, associated with prognosis. B−C. Least absolute shrinkage and selection operator (LASSO) regression analysis identifying 7 key genes (NXPH4, FAM110B, GPC2, STXBP6, CYP27B1, GARNL3, PTGER3) for the prognostic model. D. Forest plot showing hazard ratios (HR) of the 7 genes. E. Heatmap of key gene expression between high-risk and low-risk groups.

Additionally, KM curves were used to explore the relationship between the risk scores and prognosis. The results showed that high-risk patients had a significantly poorer prognosis than low-risk patients ($p<0.001$) (Figure 4A). To evaluate the model's performance, we plotted time-dependent receiver operating characteristic (ROC) curves for TCGA datasets, which predicted patient prognosis for 1, 3, and 5 years (Figure 4B). The results demonstrate that the risk model exhibits strong predictive performance, a concordance index (C-index)=0.706 (95% CI, 0.680–0.732). Moreover, the calibration curve indicates a high degree of consistency between the predicted probabilities and the actual risk (Figure 4C). To validate the robustness of the model, we performed KM analysis on the GSE13507 dataset and found that the prognosis of high-risk patients was significantly worse than that of low-risk patients ($p=0.003$), as shown in Figure 4D. Next, we predicted patient prognosis for 1, 3, and 5 years and plotted time-dependent ROC curves; the predictive performance remained relatively satisfactory (Figure 4E). Finally, the calibration curve demonstrated that the predictive probability of the model showed reasonable consistency with the actual risk (Figure 4F). In summary, the constructed prognostic model demonstrated good predictive performance in both independent datasets, effectively predicting the prognosis of patients with bladder cancer.
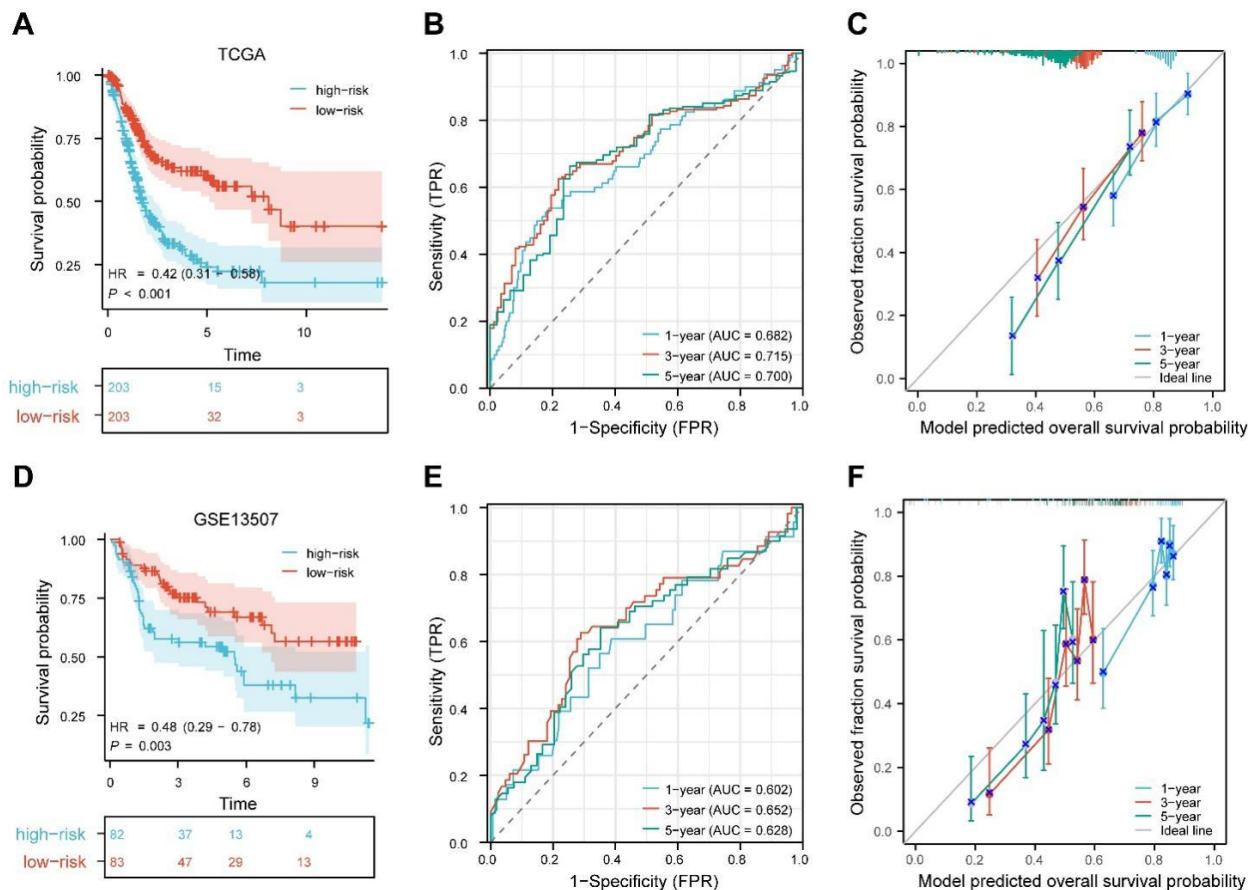

Figure 4. Evaluation of Prognostic Model Performance. A–C. Kaplan-Meier analysis was conducted on The Cancer Genome Atlas (TCGA) dataset, and time-dependent receiver operating characteristic (ROC) curves were used to assess the model's prognostic performance for 1-year, 3-year, and 5-year survival outcomes. Calibration curves were also plotted to illustrate the consistency between the model's predicted probabilities and actual risks. D–F. The robustness of the model was validated using the GSE13507 dataset, with time-dependent ROC curves and calibration curves presented to evaluate its performance and consistency.

Analysis of Key Gene Expression

Next, we analyzed the expression of feature genes in the model and plotted box plots. The results showed that compared to adjacent normal tissues, the genes GPC2 (Figure 5C), NXPH4 (Figure 5D), and CYP27B1 (Figure 5G) were upregulated in bladder cancer patients. Conversely, STXBP6 (Figure 5A), PTGER3 (Figure 5B), FAM110B (Figure 5E), and GARNL3 (Figure 5F) were downregulated in bladder cancer patients.

Survival Analysis of Key Genes

Furthermore, we used the GEPIA2 online tool to plot KM survival curves for the feature genes. The results showed that for STXBP6 (Figure 6A), NXPH4 (Figure 6C), PTGER3 (Figure 6D), and FAM110B (Figure 6G), patients with high expression levels had significantly shorter survival times than those with low expression levels. Conversely, patients with high expression levels of GPC2 have significantly longer survival times than those with low expression levels (Figure 6E). No statistically significant association was observed between the expression levels of CYP27B1 (Figure 6B) and GARNL3 (Figure 6F) and patient survival time.

Correlation between Prognostic Model and Immune Infiltration

We used the CIBERSORT algorithm to calculate the relative abundance of 22 immune cell types in bladder cancer samples and compare immune cell differences between high-risk and low-risk patients using box plots. Notably, the relative abundance of M0 and M2 macrophages was significantly higher in high-risk patients than in low-risk patients, while M1 macrophages were significantly more abundant in the low-risk group (Figure 7A). Next, we applied the ESTIMATE algorithm to calculate the ImmuneScore, StromalScore, and ESTIMATEScore for bladder cancer samples. The results showed that all three scores were lower in the high-risk group than the low-risk group (Figure 7B). Finally, Pearson's correlation analysis was used to investigate the relationship between risk scores and immune cell infiltration. The analysis identified correlations between risk scores and five immune cell types: risk scores were negatively correlated with T cells CD4 memory activated, dendritic cells resting, mast cells resting, and monocytes, and positively correlated with T cells CD4 memory resting (Figure 7C–G).

Further analysis of the sensitivity differences between these small molecules provides important clues for the personalized treatment of high-risk bladder cancer patients. For Doxorubicin and Pazopanib, the half-maximal inhibitory concentration (IC50) values were significantly higher in the high-risk group, suggesting that high-risk patients may have a stronger resistance to these drugs and poorer efficacy. In such cases, conventional doses of Doxorubicin and Pazopanib might not achieve the desired therapeutic effect, necessitating the consideration of dose adjustment or combination with other drugs. Conversely, dasatinib, erlotinib, and nilotinib showed significantly lower IC50 values in the high-risk group, indicating that high-risk patients may be more sensitive to these drugs, potentially resulting in improved therapeutic outcomes. Therefore, these drugs should be prioritized for high-risk bladder cancer patients, especially those with higher drug resistance. For Paclitaxel, there was no significant difference in IC50 between the high-risk and low-risk groups, suggesting that this drug might have similar efficacy across different risk groups and could be used in standard treatments (Figure 8A–F).
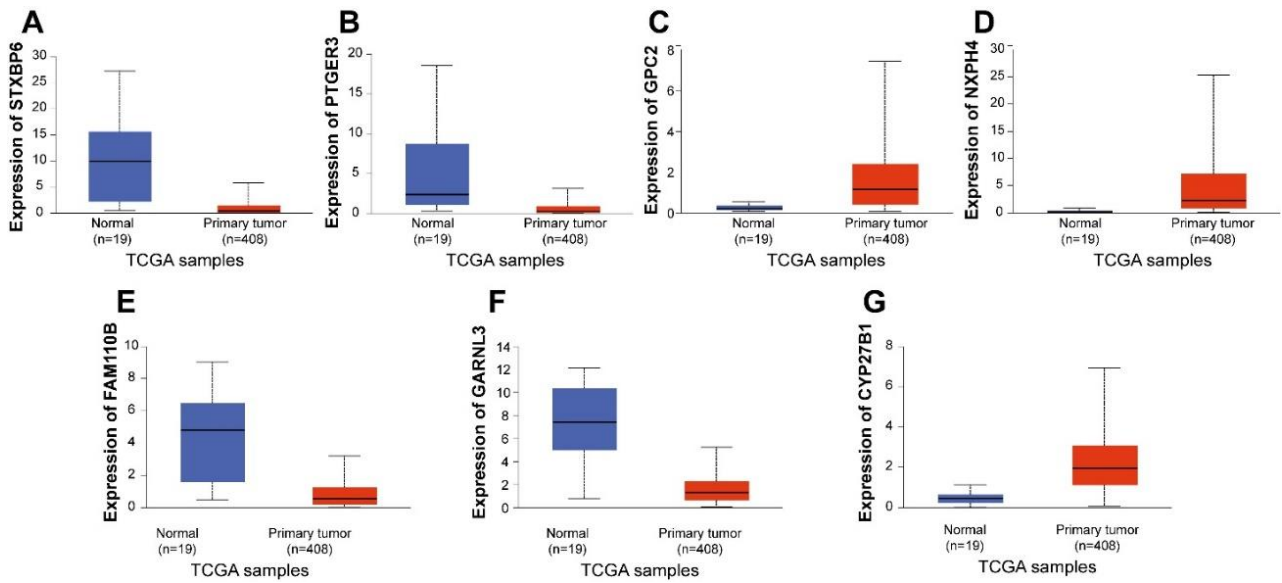
Figure 5. Expression Analysis of Key Genes. (A) Boxplot of STXBP6 expression showing downregulation in bladder cancer samples. (B) Boxplot of PTGER3 expression showing downregulation in bladder cancer samples. (C) Boxplot of GPC2 expression showing upregulation in bladder cancer samples. (D) Boxplot of NXPH4 expression showing upregulation in bladder cancer samples. (E) Boxplot of FAM110B expression showing downregulation in bladder cancer samples. (F) Boxplot of GARNL3 expression showing downregulation in bladder cancer samples. (G) Boxplot of CYP27B1 expression showing upregulation in bladder cancer samples.
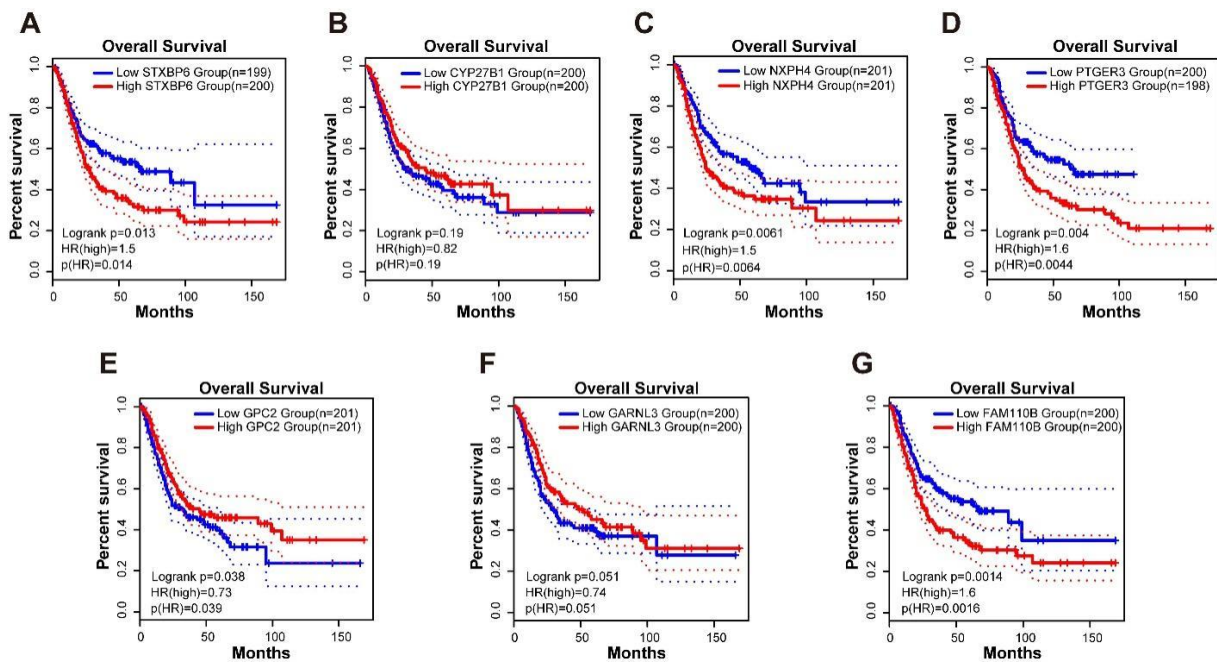

Figure 6. Survival Analysis of Feature Genes. (A) Kaplan-Meier (KM) survival curves for STXBP6. (B) KM survival curves for CYP27B1. (C) KM survival curves for NXPH4. (D) KM survival curves for PTGER3. (E) KM survival curves for GPC2. (F) KM survival curves for GARNL3. (G) KM survival curves for FAM110B.
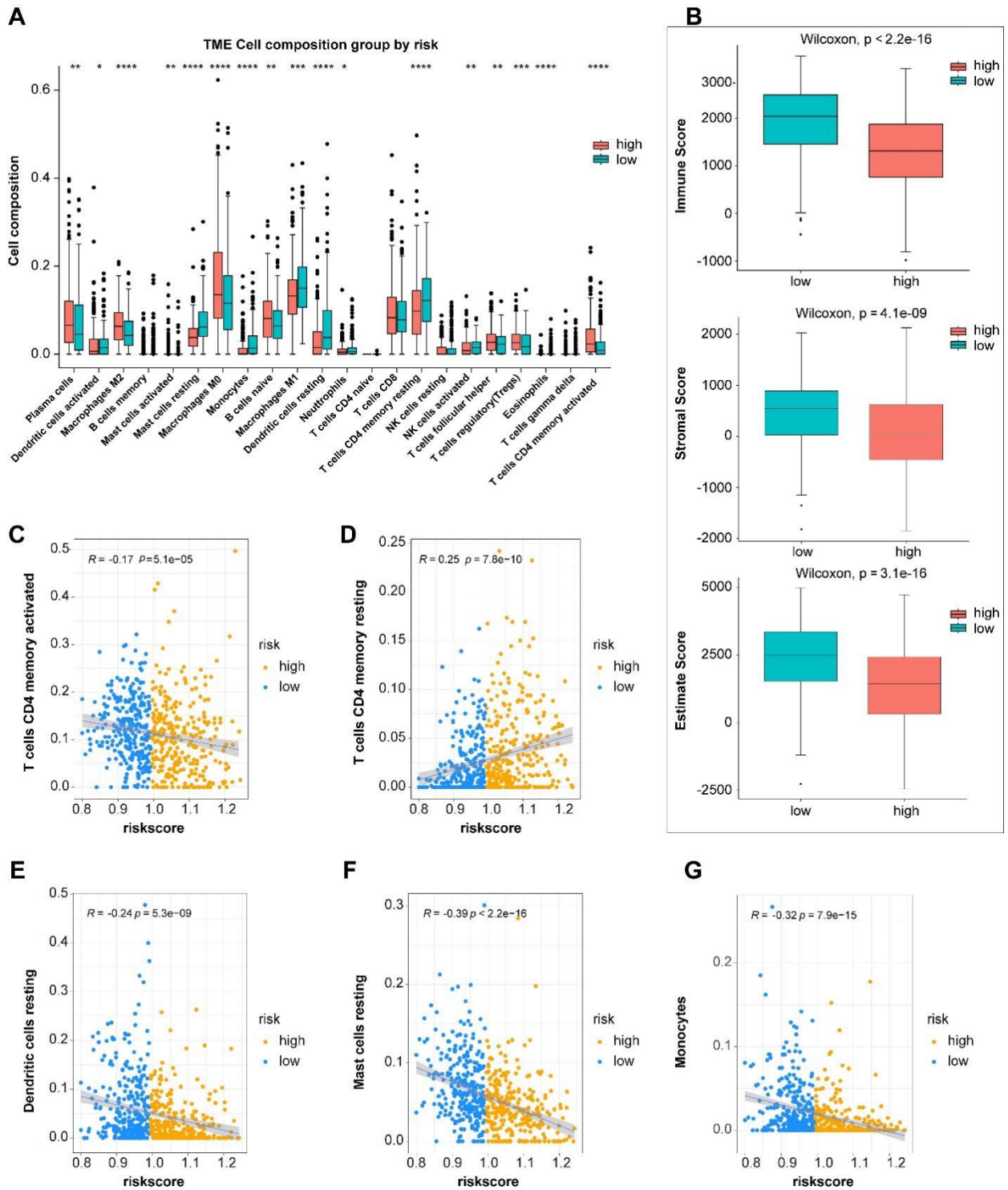
Figure 7. Correlation of Prognostic Model with Immune Infiltration. A. Boxplot comparing the relative abundance of immune cell types in high-risk versus low-risk patients. B. Boxplot showing Immune Score, Stromal Score, and ESTIMATE Score, all significantly lower in the high-risk group. C–G. Correlation analysis showing the relationship between risk score and various immune cells.
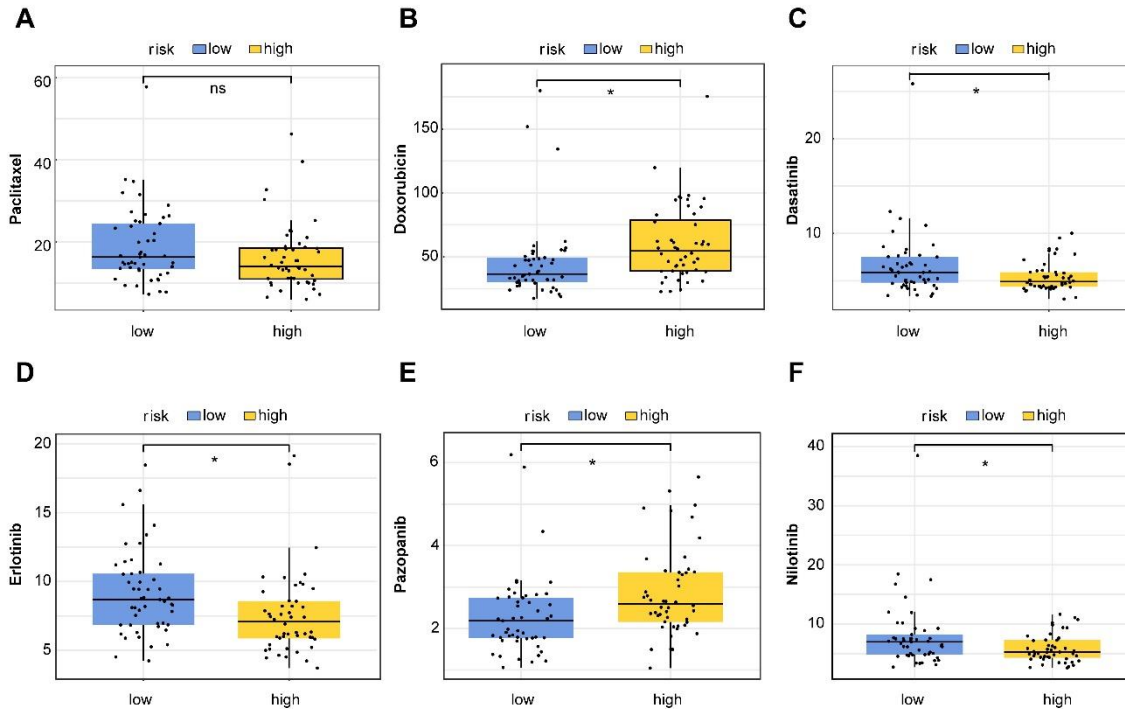
Figure 8. Sensitivity Analysis of Small Molecule Drugs. (A−F) Boxplots showing half-maximal inhibitory concentration (IC50) values of paclitaxel, doxorubicin, dasatinib, erlotinib, pazopanib, and nilotinib in high-risk versus low-risk groups.

DISCUSSION

Bladder cancer is a common malignancy of the urinary system and is characterized by high recurrence and metastatic rates. Recent advances in molecular biology techniques have significantly improved early diagnosis, prognosis assessment, and treatment monitoring of bladder cancer. Molecular biomarkers in the urine, such as fibroblast growth factor receptor 3 (FGFR3) mutations, telomerase reverse transcriptase (TERT) promoter mutations, and urine cytology, are becoming important tools for bladder cancer diagnosis.[15] Additionally, biomarkers such as E-cadherin, human epidermal growth factor receptor 2 (HER2), and microRNAs (e.g., miR-145 and miR-200c) in urine have shown potential diagnostic value.[16-18] As molecular biology techniques evolve, more biomarkers are being identified, aiding early diagnosis, prognosis evaluation, and treatment decisions for bladder cancer.

In this study, we conducted an in-depth analysis of gene expression data from TCGA bladder cancer samples and successfully identified differentially expressed bladder cancer-related genes, leading to the construction of a prognostic model. These analyses not only revealed the molecular characteristics of bladder cancer but also provided crucial information for personalized treatment strategies. First, PCA analysis of the filtered mRNA genes showed significant differences in the distribution patterns of bladder cancer and adjacent normal samples in PC1 and PC2, indicating distinct gene expression features in bladder cancer samples. Differential expression analysis identified 837 differentially expressed genes, including 238 upregulated and 599 downregulated genes. These gene expression patterns are closely related to the development of bladder cancer and provide a foundation for further functional enrichment analyses. Subsequent KEGG pathway analysis revealed that these differentially expressed genes were enriched in pathways related to cardiomyopathy, the cell cycle, cGMP-PKG signaling pathway, and vascular smooth muscle contraction. Abnormal expression of cell cycle proteins and cyclin-dependent kinases (CDKs) is a significant manifestation of disrupted cell cycle regulation in bladder cancer. For instance, Cyclin D1 and CDK4/6 are often overexpressed in bladder cancer, promoting the transition from G1 to S phase and driving excessive cell proliferation.[19] Additionally, the loss or dysfunction of cell cycle inhibitors, such as mutations or deletions in the p53 gene, impairs DNA repair capacity

and increases cancer risk.[20] Such cell cycle abnormalities not only accelerate cancer cell proliferation but are also often accompanied by genomic instability, including changes in chromosome number and gene mutations, further driving tumor development.[21] It is worth noting that the cGMP-PKG signaling pathway has garnered widespread attention in recent years due to its association with tumors. cGMP (cyclic guanosine monophosphate) regulates various cellular processes, including cell proliferation, apoptosis, migration, and angiogenesis, through its major effector molecule, PKG (cGMP-dependent protein kinase). These processes are closely linked to tumor initiation, progression, and metastasis. For example, PKG inhibits tumor cell proliferation and promotes apoptosis by suppressing Wnt/β-catenin transcription.[22]

To construct the bladder cancer prognostic model, we used the LASSO algorithm to select seven key genes (NXPH4, FAM110B, GPC2, STXBP6, CYP27B1, GARNL3, and PTGER3). These genes demonstrated good predictive performance in both the TCGA and GSE13507 datasets, indicating the high accuracy and robustness of our model for predicting bladder cancer prognosis. We then performed expression and survival analyses of the feature genes. The results showed that high expression of NXPH4 was associated with poor prognosis, suggesting that NXPH4 may play a significant role in bladder cancer progression, particularly in regulating tumor cell proliferation and invasion. According to the forest plot, NXPH4 was a risk factor. Sun et al found that a high expression of NXPH4 in bladder cancer is usually associated with a poorer prognosis. This indicates that NXPH4 may be involved in tumor progression and malignant transformation. Its upregulation is closely related to tumor proliferation, invasion, and metastasis,[23] which is consistent with our findings. Similar results were reported by Tang et al, who found that increased NXPH4 expression was associated with immune cell infiltration and poor prognosis in hepatocellular carcinoma,[24] and similar findings were observed in colorectal cancer.[25]

Immune infiltration in bladder cancer plays a critical role in the tumor microenvironment, influencing disease progression and treatment outcomes. Studies have shown that the types and quantities of tumor-infiltrating immune cells are closely associated with the prognosis of bladder cancer patients. For instance, it has been found that CD8^{+} T cells and memory-activated CD4^{+} T cells are considered protective factors, while M0 and M2 macrophages and neutrophils are regarded as adverse factors.[26] Our immune infiltration analysis revealed that the relative abundance of M0 and M2 macrophages was significantly higher in the high-risk group than the low-risk group, while M1 macrophages were downregulated. Moreover, the risk score was correlated with the abundance of various immune cells, particularly different subtypes of T cells and monocytes, which is consistent with existing research findings. For example, research has discovered that a substantial conversion of resting dendritic cells (DCs) into LAMP3^{+} dendritic cells (specific activation state) contributes to the establishment of an immunosuppressive microenvironment, thereby facilitating immune evasion.[27] This suggests that the immune microenvironment (TME) in high-risk bladder cancer patients may have substantial differences in the immune cell composition.

Tumor-associated macrophages (TAMs) in bladder cancer are also considered to be critical factors influencing disease progression. M0 macrophages are undifferentiated and can transform into M1 or M2 macrophages depending on the microenvironment.[28] M1 macrophages typically have pro-inflammatory properties and enhance anti-tumor immune responses by secreting inflammatory factors, such as tumor necrosis factor-alpha (TNF-α) and interleukin-6 (IL-6). However, the downregulation in high-risk bladder cancer patients may indicate that the tumor microenvironment is undergoing immune remodeling, affecting the efficiency of anti-tumor immune responses.[29] Conversely, M2 macrophages generally have immunosuppressive properties and promote tumor growth and metastasis by secreting anti-inflammatory factors, such as IL-10 and Transforming Growth Factor-beta (TGF-β). The study has found that macrophages that are recruited to the TME are directed to polarize towards immunosuppressive M2 phenotypes through the influence of various signaling molecules released by cancer cells. These molecules include lactic acid from tumor metabolism, a range of miRNAs and lncRNAs, CSF-1, CCL2, CCL3, CCL14, and bone morphogenetic protein 4 (BMP4).[30] In addition, the increase in M2 macrophages in high-risk patients may indicate a state of immune suppression and tumor progression.[31] Based on these observations, adjusting macrophage polarization could be a potential therapeutic strategy for enhancing antitumor immune responses. Specifically, reprogramming M2 macrophages into the M1 phenotype

may restore their antitumor functions, enhancing the effectiveness of immune checkpoint inhibitors. Moreover, targeting macrophage polarization could serve as a complementary approach to existing therapies, potentially improving patient outcomes, particularly in those with high-risk bladder cancer.

Small-molecule drug sensitivity analysis further revealed differences in drug responses among high-risk patients. Doxorubicin and pazopanib showed significantly higher IC50 values in the high-risk group, suggesting stronger resistance to these drugs. Conversely, dasatinib, erlotinib, and nilotinib showed significantly lower IC50 values in high-risk patients, potentially offering better treatment options. Therefore, adjusting drug selection and dosage is crucial for personalized treatment of high-risk bladder cancer patients.

In summary, this study constructed an effective prognostic model through systematic gene expression and functional enrichment analyses, providing new insights and potential therapeutic targets for the personalized treatment of bladder cancer. Future research should further validate these findings and explore their potential clinical applications.

STATEMENT OF ETHICS

The data in this article are from public databases and are exempt from ethical review.

FUNDING

CONFLICT OF INTEREST

The authors declare no conflicts of interest.

ACKNOWLEDGMENTS

Not applicable.

DATA AVAILABILITY

The datasets generated during and/or analyzed during the current study are available from the corresponding author via Email at liuywpwk@163.com on reasonable request.

AI ASSISTANCE DISCLOSURE

Not applicable.

REFERENCES

1. Siegel RL, Miller KD, Goding SA, Fedewa SA, Butterly LF, Anderson JC, et al. Colorectal cancer statistics, 2020. Ca-Cancer J Clin. 2020;70(3):145-64.
2. Antoni S, Ferlay J, Soerjomataram I, Znaor A, Jemal A, Bray F. Bladder Cancer Incidence and Mortality: A Global Overview and Recent Trends. Eur Urol. 2017;71(1):96-108.
3. Kamat AM, Hahn NM, Efstathiou JA, Lerner SP, Malmstrom PU, Choi W, et al. Bladder cancer. Lancet. 2016;388(10061):2796-810.
4. Babjuk M, Burger M, Comperat EM, Gontero P, Mostafid AH, Palou J, et al. European Association of Urology Guidelines on Non-muscle-invasive Bladder Cancer (TaT1 and Carcinoma In Situ) - 2019 Update. Eur Urol. 2019;76(5):639-57.
5. Powles T, Duran I, van der Heijden MS, Loriot Y, Vogelzang NJ, De Giorgi U, et al. Atezolizumab versus chemotherapy in patients with platinum-treated locally advanced or metastatic urothelial carcinoma (IMvigor211): a multicentre, open-label, phase 3 randomised controlled trial. Lancet. 2018;391(10122):748-57.
6. Hemingway H. Prognosis research: why is Dr. Lydgate still waiting? J Clin Epidemiol. 2006;59(12):1229-38.
7. Mallett S, Royston P, Waters R, Dutton S, Altman DG. Reporting performance of prognostic models in cancer: a review. Bmc Med. 2010;8:21.
8. Harrell FE: Regression Modeling Strategies: With Applications to Linear Models, Logistic and Ordinal Regression, and Survival Analysis., Regression Modeling Strategies: With Applications to Linear Models, Logistic and Ordinal Regression, and Survival Analysis, 2015.
9. Balachandran VP, Gonen M, Smith JJ, DeMatteo RP. Nomograms in oncology: more than meets the eye. Lancet Oncol. 2015;16(4):e173-80.
10. Ma Y, Sun Y, Guo H, Yang R. Tumor-associated macrophages in bladder cancer: roles and targeted therapeutic strategies. Front Immunol. 2024;15:1418131. Published 2024 Nov 13.
11. Rubio C, Munera-Maravilla E, Lodewijk I, et al. Macrophage polarization as a novel weapon in

conditioning tumor microenvironment for bladder cancer: can we turn demons into gods? Clin Transl Oncol. 2019;21(4):391-403.

12. Love M, Anders S, Huber W. Differential analysis of count data–the deseq2 package. 2014;

13. Yu G, Wang LG, Han Y, He QY. clusterProfiler: an R package for comparing biological themes among gene clusters. Omics. 2012;16(5):284-7.

14. Chen B, Khodadoust MS, Liu CL, Newman AM, Alizadeh AA. Profiling Tumor Infiltrating Immune Cells with CIBERSORT. Methods Mol Biol. 2018;1711:243-59.

15. Ye F, Wang L, Castillo-Martin M, McBride R, Galsky MD, Zhu J, et al. Biomarkers for bladder cancer management: present and future. Am J Clin Exp Urol. 2014;2(1):1-14.

16. Santoni G, Morelli MB, Amantini C, Battelli N. Urinary Markers in Bladder Cancer: An Update. Front Oncol. 2018;8:362.

17. Masson-Lecomte A, Rava M, Real FX, Hartmann A, Allory Y, Malats N. Inflammatory biomarkers and bladder cancer prognosis: a systematic review. Eur Urol. 2014;66(6):1078-91.

18. Mitra AP, Datar RH, Cote RJ. Molecular pathways in invasive bladder cancer: new insights into mechanisms, progression, and target identification. J Clin Oncol. 2006;24(35):5552-64.

19. Mitra AP, Hansel DE, Cote RJ. Prognostic value of cell-cycle regulation biomarkers in bladder cancer. Semin Oncol. 2012;39(5):524-33.

20. Shangary S, Wang S. Small-molecule inhibitors of the MDM2-p53 protein-protein interaction to reactivate p53 function: a novel approach for cancer therapy. Annu Rev Pharmacol. 2009;49(12):223-41.

21. Fassl A, Geng Y, Sicinski P. CDK4 and CDK6 kinases: From basic science to cancer therapy. Science. 2022;375(6577):eabc1495.

22. Piazza GA, Ward A, Chen X, Maxuitenko Y, Coley A, Aboelella NS, et al. PDE5 and PDE10 inhibition activates cGMP/PKG signaling to block Wnt/β-catenin transcription, cancer cell growth, and tumor immunity. Drug Discov Today. 2020;25(8):1521-1527.

23. Sun X, Xin S, Jin L, Zhang Y, Ye L. Neurexophilin 4 is a prognostic biomarker correlated with immune infiltration in bladder cancer. Bioengineered. 2022;13(5):13986-99.

24. Tang Q, Chen YM, Shen MM, Dai W, Liang H, Liu JN, et al. Increased Expression of NXPH4 Correlates with Immune Cell Infiltration and Unfavorable Prognosis in Hepatocellular Carcinoma. J Oncol. 2022;2022:5005747.

25. Sun Z, Wang H, Xu Y, Liu Y, Wang L, Zhou R, et al. High expression of NXPH4 correlates with poor prognosis, metabolic reprogramming, and immune infiltration in colon adenocarcinoma. J Gastrointest Oncol. 2024;15(2):641-67.

26. Lv Y, Jin P, Chen Z, Zhang P. Characterization of hazard infiltrating immune cells and relative risk genes in bladder urothelial carcinoma. Am J Transl Res. 2020;12(11):7510-7527.

27. Li J, Jiang Y, Ma M, et al. Epithelial cell diversity and immune remodeling in bladder cancer progression: insights from single-cell transcriptomics. J Transl Med. 2025;23(1):135.

28. Mantovani A, Biswas SK, Galdiero MR, Sica A, Locati M. Macrophage plasticity and polarization in tissue repair and remodelling. J Pathol. 2013;229(2):176-85.

29. Xu Y, Wang X, Liu L, Wang J, Wu J, Sun C. Role of macrophages in tumor progression and therapy (Review). Int J Oncol. 2022;60(5):1-19.

30. Sharifi L, Nowroozi MR, Amini E, Arami MK, Ayati M, Mohsenzadegan M. A review on the role of M2 macrophages in bladder cancer; pathophysiology and targeting. Int Immunopharmacol. 2019;76(18):105880.

31. Leblond MM, Zdimerova H, Desponds E, Verdeil G. Tumor-Associated Macrophages in Bladder Cancer: Biological Role, Impact on Therapeutic Response and Perspectives for Immunotherapy. Cancers. 2021;13(18):4712.